Mechanical Multibody Systems with Deformable Components

Peter Rentrop, Oliver Scherf, and Bernd Simeon

TU Darmstadt, FB Mathematik, Schloßgartenstr. 7, D-64289 Darmstadt

Abstract. The multibody system approach provides enhanced models of vehicles, robots, and air- and spacecrafts. Mixed systems consisting of both rigid and deformable bodies are aimed at growing demands for refined simulation. A basic modeling framework for this class of mechanical systems is presented which covers also inelastic material behavior. Moreover, the Differential-Algebraic Equations (DAEs) obtained from semidiscretization in space are classified and the application of DAE solvers is discussed. Two examples illustrate the simulation tasks and show the state-of-the-art in this field of scientific computing.

1 Introduction

Constrained mechanical systems including both rigid and deformable bodies are a focus of current research in computational mechanics. These mixed systems, so-called *flexible multibody systems*, meet the increasing demand for refined simulation in vehicle dynamics, robotics, and in air- and spacecraft technology [17]. In future, the behavior of new smart materials must also be taken into account.

Elastic or inelastic bodies are described by Cauchy's first law of motion and a specific material law while rigid bodies and their interaction are usually treated by Lagrangian mechanics. Combined systems represent thus a class of mixed hyperbolic PDEs and DAEs where many questions remain open. On the other hand, today's simulation packages are able to generate a semidiscretized formulation where the deformable members of the multibody system have been discretized in space.

This paper presents a basic modeling framework for such mixed mechanical systems, covering rigid, elastic and also inelastic bodies. Moreover, the DAEs obtained from semidiscretization are classified and the application of DAE solvers is discussed. Finally, two examples illustrate the simulation tasks and show the state-of-the-art in this field of scientific computing.

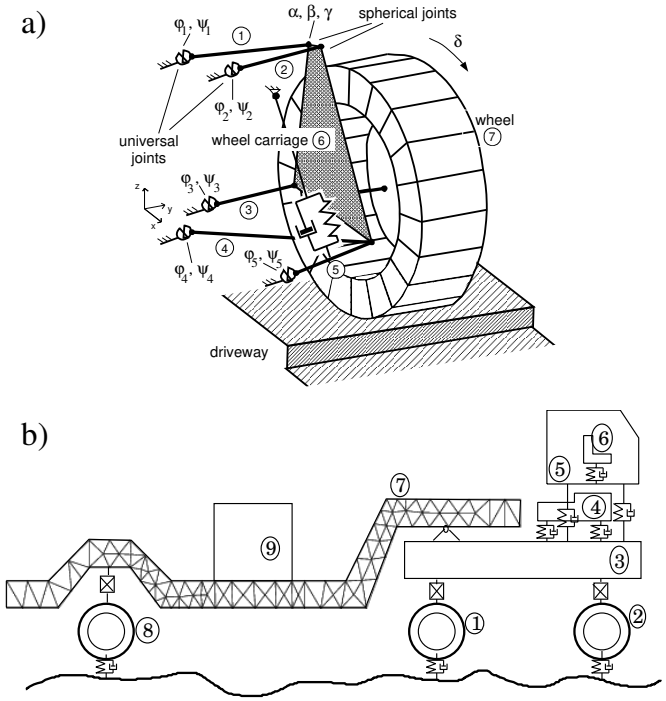

Fig. 1. Examples of multibody systems. a) Spatial wheel suspension with 7 rigid bodies, b) planar truck with 8 rigid and one elastic body (load area).

2 Rigid body systems

A multibody system consists of several interconnected bodies. Joints constrain the relative motion of pairs of bodies while springs and dampers act as compliant elements. Going back to Euler and Lagrange, this modeling approach has been originally developed for systems of rigid bodies, but extensions cover now also deformable bodies. Examples of multibody models from vehicle dynamics are shown in Fig. 1.

To provide a basic setting, we outline first the equations of motion of rigid body systems. The dynamic behavior of such constrained mechanical systems

is modeled by the Euler-Lagrange equations [15]

$$\begin{aligned} M(p)\,\ddot{p} &= f(p,\dot{p},t) - G(p)^T\lambda \\ 0 &= g(p) \end{aligned} \tag{1}$$

where, for given time t, the vector $p(t) \in \mathbb{R}^{n_p}$ specifies the position and orientation of all bodies, $\dot{p}(t)$ denotes the time-derivative of $p(t)$, and $\lambda(t) \in \mathbb{R}^{n_\lambda}$ is the vector of Lagrange multipliers. The mappings $f : \mathbb{R}^{n_p} \times \mathbb{R}^{n_p} \times [t_0, t_f] \to \mathbb{R}^{n_p}$ and $g : \mathbb{R}^{n_p} \to \mathbb{R}^{n_\lambda}$ define forces and holonomic constraints, $M(p) \in \mathbb{R}^{n_p \times n_p}$ is the symmetric, positive definite mass matrix and $G = dg/dp$ the Jacobian of the constraints, which is assumed to have full rank n_λ. This rank assumption holds for well-specified technical systems with non-redundant constraints.

The DAE (1) is of index 3, which follows directly if we differentiate the constraint $0 = g(p)$ twice,

$$0 = d/dt\, g(p) \;=\; G(p)\,\dot{p}, \qquad 0 = d^2/dt^2 g(p) \;=\; G(p)\,\ddot{p} + G_p(p)(\dot{p},\dot{p})\,. \tag{2}$$

The dynamic equation for $\ddot{p}$ in (1) and the second constraint derivative yield

$$Q(p)\begin{pmatrix}\ddot{p}\\ \lambda\end{pmatrix} = \begin{pmatrix} f(p,\dot{p},t) \\ -G_p(p)(\dot{p},\dot{p}) \end{pmatrix}, \quad Q(p) := \begin{pmatrix} M(p) & G(p)^T \\ G(p) & 0 \end{pmatrix}, \tag{3}$$

where the matrix $Q(p)$ is regular. Thus, we can solve for the Lagrange multipliers λ, and the differential index equals 3. Various numerical algorithms for the Euler-Lagrange equations (1) have been developed in the last decade, see e.g. [6,8,19]. In the next section, it is shown that the basic structure of the equations is preserved if elastic bodies enter the system. However, there appears an additional partitioning of unknowns into gross motion coordinates and deformation variables.

3 Elastic bodies

We start with the single body elastic motion to provide an appropriate framework for the treatment of mixed systems. Consider the continuum body in Fig. 2. It forms a compact domain in Euclidean space whose configuration at time t is determined by the position of its material points. Each material point can be identified by its position $x \in \overline{\Omega}$ where $\Omega \subset \mathbb{R}^3$ is the open interior of a reference configuration. For the moment, we assume the reference configuration to be expressed in the inertial coordinate system e_I.

The deformation φ is a vector field which locates the material points depending on reference configuration and time, $\varphi : \overline{\Omega} \times [t_0,\, t_f] \to \mathbb{R}^3$, $(x,t) \mapsto$

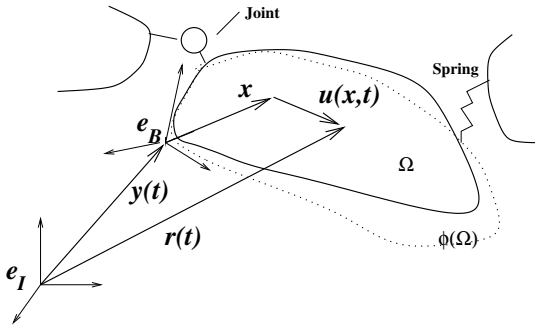

Fig. 2. Deformable body and reference frames.

$\varphi(x,t)$. Equivalently, the configuration is described by the displacement field $u(x,t) = \varphi(x,t) - x$. With the deformation gradient denoted by $\nabla\varphi = \partial\varphi/\partial x$, the Green-St.Venant strain tensor

$$E(\nabla\varphi) = \frac{1}{2}(\nabla\varphi^T\nabla\varphi - I) = \frac{1}{2}(\nabla u + \nabla u^T + \nabla u^T\nabla u)$$

measures deformation independently of translation and rotation.

Cauchy's first law of motion characterizes the deformed body. Expressed in the reference configuration, it reads in strong form, Ciarlet [5],

$$\rho\ddot{u} = \beta + \text{div } P \qquad \text{in } \Omega \tag{4}$$

$$u = \bar{u} \qquad \text{on } \Gamma_0 \tag{5}$$

$$Pn = \bar{\tau} \qquad \text{on } \Gamma_1 \tag{6}$$

where $\rho(x,t)$ denotes the mass density, $\beta(x,t)$ the density of body forces, $P(x,t)$ the first Piola-Kirchhoff stress tensor, $\bar{u}(x,t)$ the geometric or essential boundary conditions, and $\bar{\tau}(x,t)$ the surface tractions or natural boundary conditions. The unit normal vector n is supposed to exist almost everywhere on the boundary $\partial\Omega = \overline{\Gamma_0 \cup \Gamma_1}, \Gamma_0 \cap \Gamma_1 = \emptyset$. Instead of the unsymmetric tensor P, the symmetric second Piola-Kirchhoff stress tensor $\Sigma = \nabla\varphi^{-1}P$ is commonly used. Analogously to the principle of virtual work, the weak form of the hyperbolic PDE (4) is

$$\int_\Omega v^T\rho\ddot{u}\,dx = \int_\Omega v^T\beta\,dx - \int_\Omega P : \nabla v\,dx + \int_{\Gamma_1} v^T\bar{\tau}\,da \tag{7}$$

for all test functions $v : \overline{\Omega} \to \mathbb{R}^3, v|_{\Gamma_0} = 0$. Here, $A : B = \text{tr}(AB^T)$ denotes the dot product of second order tensors (or matrices) A and B.

The equations of motion (7) lack a material law relating stress Σ (or P) and strain E. For ease of presentation, we concentrate in this section on linearized elasticity where second order strain terms are neglected and

$$\varepsilon(\nabla u) = (\nabla u + \nabla u^T)/2 \tag{8}$$

is employed as strain measure instead of E. Then, $\int_\Omega P : \nabla v \, dx$ in (7) is replaced by $\int_\Omega \underline{\sigma}^T \underline{\varepsilon} \, dx$ where $\underline{\varepsilon}$ and $\underline{\sigma}$ denote vectors comprising the 6 essential components of strain and stress [9]. Hooke's law relates both by

$$\underline{\sigma} = D \, \underline{\varepsilon} \tag{9}$$

with the constant 6×6 matrix D depending on Young's modulus and Poisson's number. In Sect. 4, this material law will be extended to the viscoplastic case.

For space discretization, we reformulate the weak form (7) in an appropriate Sobolev space, Hughes [9]. The test functions are elements of

$$\mathcal{V} = \left\{ v \in H^1(\Omega, \mathbb{R})^3 : \, v|_{\Gamma_0} = 0 \right\} \tag{10}$$

and the solution $u(\cdot, t)$, for time t fixed, is element of

$$\mathcal{S}_t = \left\{ u(\cdot, t) \in H^1(\Omega, \mathbb{R})^3 : \, u(\cdot, t)|_{\Gamma_0} = \bar{u}(\cdot, t) \right\}. \tag{11}$$

The usual formal setting is based on the scalar product inducing the energy norm

$$a(u, v) := \int_\Omega \underline{\varepsilon}(\nabla u)^T D \underline{\varepsilon}(\nabla v) \, dx$$

and the integrals $(v, \beta) := \int_\Omega v^T \beta \, dx$, $(v, \bar{\tau})_\Gamma := \int_{\Gamma_1} v^T \bar{\tau} \, da$. Given initial data $u(x, t_0)$ and $\dot{u}(x, t_0)$, the weak form (7) then reads: *Find* $u(\cdot, t) \in \mathcal{S}_t$, $t \in [t_0, t_f]$, *such that for all* $v \in \mathcal{V}$

$$(v, \rho \ddot{u}) = (v, \beta) - a(u, v) + (v, \bar{\tau})_\Gamma. \tag{12}$$

The associated discrete problem follows by choosing an N-dimensional subspace $\mathcal{V}_\Delta \subset \mathcal{V}$ and setting

$$u(x, t) \doteq q_0(x, t) + \sum_{i=1}^{N} v_i(x) q_i(t), \qquad q_0(\cdot, t)|_{\Gamma_0} = \bar{u}(\cdot, t), \;\; v_i \in \mathcal{V}_\Delta. \tag{13}$$

Finally, we insert the ansatz for u in (12), apply the test functions v_i, $i = 1, \ldots, N$, and obtain a system of second order ordinary differential equations for the unknown coefficients $q = (q_1, \ldots, q_N)$, the *equations of structural dynamics* [9]

$$M_\Delta \ddot{q} = -K_\Delta q + b(t) \tag{14}$$

with mass matrix $M_\Delta = ((v_i, \rho v_j))_{i,j=1}^N$, stiffness matrix $K_\Delta = (a(v_i, v_j))_{i,j=1}^N$, and force vector $b(t) = ((v_i, \beta - \rho\ddot{q}_0) - a(v_i, q_0) + (v_i, \bar{\tau})_\Gamma)_{i=1}^N$. Note that the often employed Rayleigh damping leads to an additional term $-D_\Delta \dot{q}$ on the right hand side of (14), with damping matrix $D_\Delta = \alpha_1 M_\Delta + \alpha_2 K_\Delta$.

Taking the gross motion into account. So far, we have derived a well-known model for a single body's small elastic deformation. In a multibody system, however, each component may perform rotation and translation in space, and accordingly we need additional coordinates to track this *gross motion*. In other words, the overall motion is now split into gross motion plus small deformation. The latter is conveniently expressed in a body-fixed reference frame [10,23].

Let e_B denote the reference frame attached to the body and e_I the inertial frame, Fig. 2. Then each material point is located by vector

$$r(t) = y(t) + A(\phi(t))(x + u(x,t)) \tag{15}$$

where $y(t) \in \mathbb{R}^3$ specifies the origin of e_B in terms of e_I, $A(\phi(t))$ denotes the 3×3 direction cosine matrix of e_B relative to e_I, and material point x and displacement $u(x,t)$ refer to e_B [10]. The matrix A depends on three angles $\phi(t) = (\phi_1(t), \phi_2(t), \phi_3(t))$. Singularities can be avoided by taking four Euler parameters instead, see [15]. Differentiating r and introducing the angular velocity $\omega(t) = (\omega_1(t), \omega_2(t), \omega_3(t))$ with respect to e_B, one obtains

$$\ddot{r} = \ddot{y} + A(\phi)(\tilde{\dot{\omega}} + \tilde{\omega}\tilde{\omega})(x + u) + 2A(\phi)\tilde{\omega}\dot{u} + A(\phi)\ddot{u}$$

with the skew symmetric matrix $A(\phi)^T \frac{d}{dt} A(\phi) = \tilde{\omega} := \begin{pmatrix} 0 & -\omega_3 & \omega_2 \\ \omega_3 & 0 & -\omega_1 \\ -\omega_2 & \omega_1 & 0 \end{pmatrix}$.

The principle of virtual work (7) also characterizes the body in terms of r where the admissible test functions are now restricted to the tangent space of the motion r with time t held fixed [5,10,24]. We skip the straightforward but tedious computations and state only the final form of the semidiscretized equations of motion. The displacement u is defined as linear combination of test functions v_i as in (13). The equations for y and ω read

$$\begin{aligned} m\ddot{y} + A\tilde{s}^T\dot{\omega} + A\tilde{\omega}\tilde{\omega}s + A\int \rho(2\tilde{\omega}\dot{u} + \ddot{u})dx &= \int \beta\, dx + \int \bar{\tau}\, da \\ \tilde{s}A^T\ddot{y} + J\dot{\omega} + \tilde{\omega}J\omega + \int \rho(\tilde{x} + \tilde{u})\ddot{u}\, dx &= \int (\tilde{x} + \tilde{u})A^T\beta\, dx \\ &\quad + \int (\tilde{x} + \tilde{u})A^T\bar{\tau}da - \int 2\rho(\tilde{x} + \tilde{u})\tilde{\omega}\dot{u}\, dx \end{aligned} \tag{16}$$

with body mass $m = \int \rho\, dx$, 3×3 inertia matrix $J = -\int \rho(\tilde{x} + \tilde{u})(\tilde{x} + \tilde{u})\, dx$, and $s = \int \rho(x + u)\, dx$. If the origin of the body-fixed reference frame is

placed in the centroid $c = s/\rho$, it holds $s = 0$. Moreover, in case of vanishing deformation $u \equiv 0$, (16) reduces to the Newton-Euler equations

$$m\ddot{y} = F_A, \qquad J\dot{\omega} + \tilde{\omega} J\omega = M_A \tag{17}$$

of a rigid body with applied forces and moments F_A and M_A.

The deformation is given by

$$\begin{aligned}(v_i, \rho A^T \ddot{y}) + (v_i, \rho(\tilde{\dot{\omega}} + \tilde{\omega}\tilde{\omega})(x+u)) + (v_i, \rho(2\tilde{\omega}\dot{u} + \ddot{u})) \\ = (v_i, A^T\beta) - a(u, v_i) + (v_i, A^T\bar{\tau})_\Gamma, \qquad i = 1, \ldots, N.\end{aligned} \tag{18}$$

For vanishing gross motion $y \equiv 0$ and $\phi \equiv 0$, (18) coincides with the equations of structural dynamics (14). Collecting some terms in (16) and (18), we can rewrite the equations of single body elastic motion as, cf. [10,23],

$$\begin{pmatrix} \begin{pmatrix} m & A_\phi \tilde{s}(q)^T \\ \tilde{s}(q) A_\phi^T & J(q) \end{pmatrix} & C(\phi, q)^T \\ C(\phi, q) & M_\Delta \end{pmatrix} \begin{pmatrix} \ddot{y} \\ \dot{\omega} \\ \ddot{q} \end{pmatrix} = b(y, \phi, \omega, q, \dot{q}, t) - \begin{pmatrix} 0 \\ 0 \\ K_\Delta\, q \end{pmatrix} \tag{19}$$

where q denotes again the deformation or node variables, C coupling terms in the mass matrix, and b comprises body forces, surface tractions, and generalized centrifugal and Coriolis forces.

The semidiscretized eqs. (19) are often written as purely second order system using some generalized gross motion variables p and velocities $\dot{p}$ instead of y, ϕ and ω. While most elastic bodies in multibody systems satisfy the mathematical model presented here, there are applications where additional nonlinear elasticity terms are required, e.g., if *geometric stiffening* of slim bodies is taken into account [23]. The term $-K_\Delta q$ is then replaced by $-\nabla W_\Delta(q)$ with elastic potential $W_\Delta(q)$.

Assembling the multibody system equations. Several simulation packages apply a two stage process to generate the equations of motion of elastic multibody systems [17]. First, the elastic bodies are semidiscretized as described above, e.g., by a finite element code, and then all corresponding data like mass and stiffness matrices as well as additional integrals are imported into a multibody code. With respect to the overall system, the semidiscretized elastic body (19) represents thus one type of component, the others being rigid bodies, springs, dampers, actuators, and joints.

Coupling forces between an elastic and another body induced, e.g., by a spring, are expressed in terms of the surface traction $\bar{\tau}$, which now depends on the motion of both bodies. Taking these forces into account, an automatic assembly loop connects finally all components and generates the equations

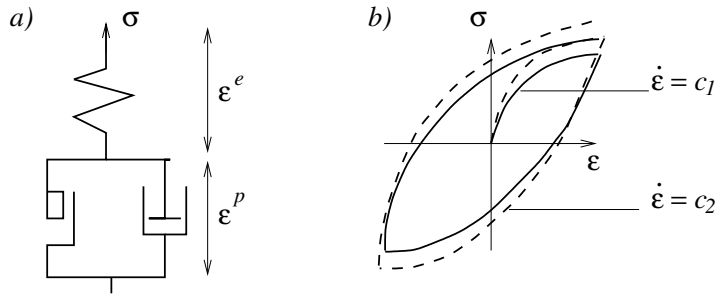

Fig. 3. Viscoplastic material. a) Rheologic model, b) stress-strain diagram.

of motion in the same fashion as in the rigid body case (1). We just give the equations in a general form where p comprises all gross motion coordinates and q all deformation variables of possibly several elastic bodies. Basically, the same structure as in the purely rigid body case is obtained:

$$\begin{pmatrix} M(p,q) & C(p,q)^T \\ C(p,q) & M_\Delta \end{pmatrix} \begin{pmatrix} \ddot{p} \\ \ddot{q} \end{pmatrix} = \begin{pmatrix} f(p,\dot{p},q,\dot{q},t) \\ b(p,\dot{p},q,\dot{q},t) - K_\Delta q \end{pmatrix} - G(p,q)^T\lambda \qquad (20)$$
$$0 = g(p,q)$$

Note that M_Δ, K_Δ, C and b may also stand for several elastic bodies. Moreover, M, f and g coincide with the rigid system (1) for vanishing deformation.

It should be stressed that the mathematical model outlined so far leaves several questions open. The original problem is a mixed DAE-PDE or PDAE system, Campbell/Marszalek [3], whose structure is hidden in the semidiscretized equations (20). On the other hand, FE methods express constraints like contact conditions often as saddle point problems and solve them by mixed discretizations, Kikuchi/Oden [11], with the surface tractions $\bar{\tau}$ playing the role of Lagrange multipliers. Such approaches are, however, still too expensive in multibody simulations where joints are ideal, frictionless interconnections without any elasticity.

For a given space discretization, the differential index of the partitioned DAE (20) is again 3, like in the rigid body case, if the constraints are not redundant, i.e., rank $G(p,q) = n_\lambda = \text{full}$. This follows directly by differentiation, cf. the rigid body constraint derivatives (2). It is not clear so far how to generalize the perturbation index [8] to such mixed systems. Error estimates in time for perturbed solutions of (20) will obviously involve the underlying space discretization function space $\mathcal{V}_\Delta$.

4 Inelastic bodies

The mathematical models presented above suffice in many applications. Aspects like long term material behavior and material wear, however, require a more general approach. We concentrate in this section on the large class of *viscoplastic materials* and derive an extended multibody system formulation which includes both elastic and inelastic bodies.

Viscoplastic material behavior is characterized by the rheologic model of Fig. 3 a). The spring stands for the elastic part of the stress-strain relation while the damper and the friction elements represent inelastic effects. In particular, the damper involves a time dependency, i.e., the stress σ depends on the *rate* $\dot{\varepsilon}$. Fig. 3 b) shows the corresponding stress-strain diagram with its typical hysteresis effect for cyclic loading.

Among the various approaches for viscoplastic material laws, we follow here [2] and assume an additive decomposition of total strain ε into elastic strain ε^e and plastic strain ε^p,

$$\varepsilon = \varepsilon^e + \varepsilon^p \; . \tag{21}$$

Here, ε is given by the symmetric part (8) of the displacement gradient, ε^e satisfies an elastic material law, and ε^p is defined by a set of *evolution equations* to be expressed below. Thus, the ansatz (21) generalizes the elastic behavior to the plastic case and leads to a *macro model* or a phenomenologic description. Extensive tests and experimental identification have to be performed to obtain sufficiently accurate data for such macro models [18]. *Micro models* on the level of the crystal structure, on the other hand, resolve the material at hand better but are still much too expensive to be applied to 2D or 3D bodies in a large scale.

As in Section 3, we restrict the discussion to small displacements. Due to Hooke's law (9) for ε^e and the decomposition (21), the stress can be written in vector notation as

$$\underline{\sigma} = D\,(\underline{\varepsilon} - \underline{\varepsilon}^p), \tag{22}$$

and, accordingly, the weak form of the balance equations (7) reads in the viscoplastic case [7]

$$(v, \rho\ddot{u}) = (v, \beta) - a(u, v) + \int_\Omega \underline{\varepsilon}^{p^T} D\underline{\varepsilon}(\nabla v)\, dx + (v, \bar{\tau})_\Gamma \tag{23}$$

for all test functions $v \in \mathcal{V}$ defined in (10). In each material point x, the plastic strain ε^p satisfies evolution equations

$$\dot{\varepsilon}^p = \Phi(\sigma, \zeta), \qquad \dot{\zeta} = \Psi(\sigma, \zeta) \; , \tag{24}$$

Table 1. Overview of different models

Bodies	*(Semidiscretized) Equations of Motion*	*Index*
rigid	$M(p)\,\ddot{p} = f(p,\dot{p},t) - G(p)^T\lambda$ $0 = g(p)$	3
rigid + elastic	$\boldsymbol{M}(\cdot)\begin{pmatrix}\ddot{p}\\ \ddot{q}\end{pmatrix} = \begin{pmatrix} f(\cdot,t)\\ b(\cdot,t) - K_\Delta q\end{pmatrix} - G(p,q)^T\lambda$ $0 = g(p,q)$	3
rigid + elastic/ viscoplastic	$\boldsymbol{M}(\cdot)\begin{pmatrix}\ddot{p}\\ \ddot{q}\end{pmatrix} = \begin{pmatrix} f(\cdot,t)\\ b(\cdot,t) - K_\Delta q + C_\Delta w\end{pmatrix} - G(p,q)^T\lambda$ $\dot{w} = \Phi(q,w,z)$ $\dot{z} = \Psi(q,w,z)$ $0 = g(p,q)$	3
single body viscoplastic long term load	$0 = -K_\Delta q + C_\Delta w + b(t)$ $\dot{w} = \Phi(q,w,z)$ $\dot{z} = \Psi(q,w,z)$	1

where Φ and Ψ denote *flow* and *hardening rules* and the internal variables ζ can be either scalars or second order tensors. Concerning existence and uniqueness of solutions of such mixed systems (22) to (24), we refer to recent results of Alber [1].

If (23) is discretized in space, the additional integral due to the plastic strain has to be computed numerically. For this reason, values of both ε^p and ζ are required at all quadrature points ξ of the grid. Let vector $w(t)$ comprise the discrete values of $\varepsilon^p(\xi,t)$ in the quadrature points and vector $z(t)$ the analogue values of $\zeta(\xi,t)$. Then, the semidiscretized equations of motion take the form, c.f. (14),

$$M_\Delta\ddot{q} = -K_\Delta q + C_\Delta w + b(t) \tag{25}$$

where C_Δ is the matrix resulting from the quadrature rule. The evolution equations are only evaluated in the quadrature points and read, with the stresses replaced by the discrete analogue of (22),

$$\dot{w} = \Phi(q,w,z), \qquad \dot{z} = \Psi(q,w,z)\,. \tag{26}$$

In the same fashion as before in Sect. 3, this semidiscretized single body model can be incorporated in a multibody system. We obtain then a DAE

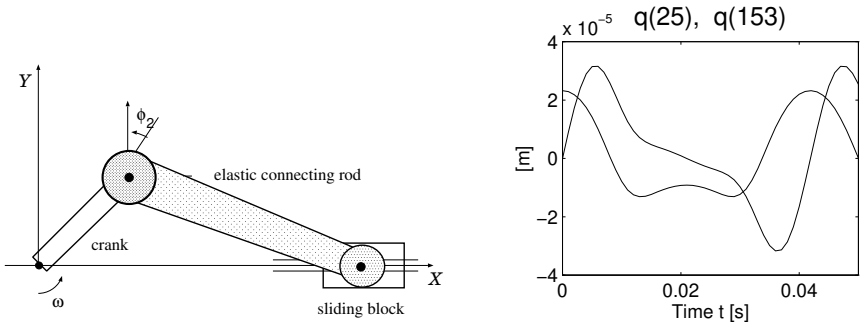

Fig. 4. Slider crank, displacements of connecting rod at midpoint and right joint.

of the form (20) with additional differential equations for plastic strain and internal variables, see the overview in Table 1. The differential index equals again 3 as no additional constraints enter the equations. Table 1 includes also a special case which is important in single body inelastic simulation. If only long term behavior is of interest, e.g., in the simulation of tensile tests, the acceleration term on the left of (25) is often neglected. With the stiffness matrix K_Δ being regular, an index 1 system has then to be solved.

5 Simulation examples

At first sight, the time integration of the DAEs presented above seems an easy task since various successful methods have been developed in the last decade [6,19]. Though index 3 problems should not be solved directly due to ill-conditioning and order reduction, there are techniques available which lead to stabilized formulations of lower index [8]. But - except for rigid body systems - one should not look at these DAEs from a pure time integration point of view, neglecting in this way the space discretization with its strong influence on the solution behavior. In fact, it turns out that the high frequencies induced by the deformable bodies lead to a singularly perturbed or *stiff mechanical system* in time. Otherwise excellent methods like the implicit Runge-Kutta method RADAU5 [8] may suffer then from severe order reduction and from ill-conditioned iteration matrices [12]. Hence, the interplay of space and time discretization needs further attention, see [14] for first results. Two examples illustrate the situation in the following.

Slider crank. The slider crank benchmark problem [10,20] consists of two rigid bodies, crank and sliding block, and an elastic connecting rod, Fig. 4.

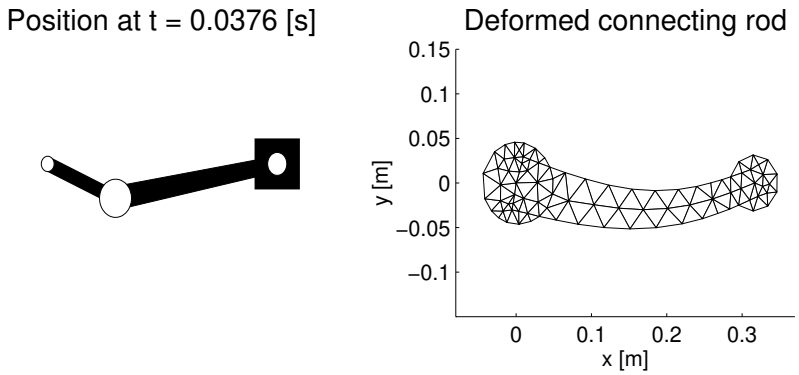

Fig. 5. Slider crank, deformed mesh (scaled by 10^3).

The crank motion is prescribed with constant angular velocity $\omega = 150$[rad/s]. The finite element grid and corresponding data like mass and stiffness matrices M_Δ and K_Δ were generated by means of the Matlab PDE toolbox [13], with a total of 176 deformation or node variables describing the lateral and longitudinal displacement of the elastic body. Fig. 5 shows a snapshot of a simulation result obtained by time integration of the index 2 formulation of the DAE (20) by RADAU5. Here, it is very important to provide consistent initial values close to the smooth or essentially non-oscillatory motion, in particular for the longitudinal deformation. Additionally, only low tolerances can be prescribed for both velocities and accelerations of the deformation variables since otherwise the effect of order reduction forces the code to take very small steps though the solution is smooth.

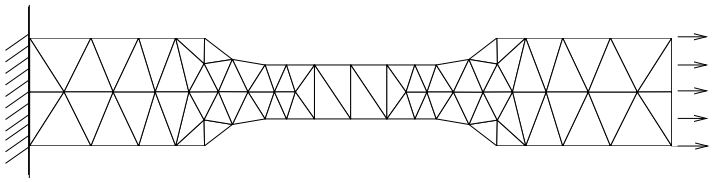

Fig. 6. Tensile test of viscoplastic bolt.

Tensile test of a viscoplastic bolt. The second example is a 2D simulation of a bolt in a tensile test, Fig. 6. This single body viscoplastic model demon-

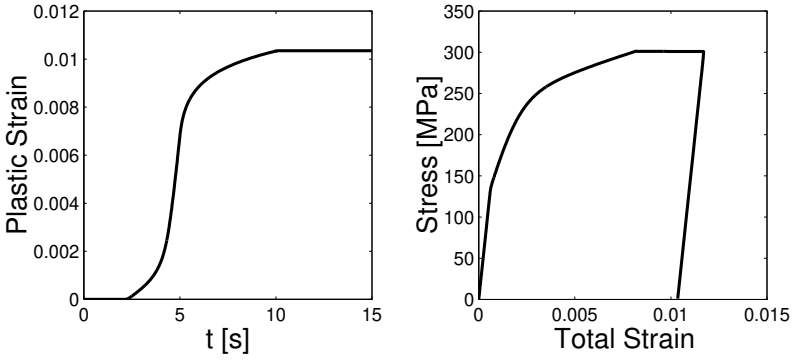

Fig. 7. Simulation result, plastic strain ϵ_{11}^p and stress-strain relation $\epsilon_{11}/\sigma_{11}$.

strates some basic effects in inelastic material behavior. After a stretching phase, the bolt is held fixed and finally the load decreases again. We use the model of Chan-Bodner-Lindholm [4] for the stainless steel SS316 (nickel-chromium, single crystal) with the parameters of [18] in a plane stress simulation. The bolt was discretized by 6 node triangular finite elements and second order Gaussian quadrature. For this particular system, 12 displacement variables q and a total of 30 additional internal variables w and z arise per element. Fig. 7 shows plastic strain versus time and the stress-strain diagram for the time dependent surface load. Assuming quasistatic behavior, i.e., neglecting the acceleration term on the left of (25), the BDF-2 method was used to integrate the semidiscretized equations of motion. The index 1 system to be solved here poses special difficulties due to its large dimension and the numerical stiffness of the evolution equations [7]. We supplied an analytic Jacobian computation to stabilize and speed up the nonlinear system solution and applied a standard predictor-corrector scheme [21] for stepsize control. Further details on this particular benchmark problem and on the time integration scheme can be found in [16].

Acknowledgement: The authors gratefully acknowledge the support by German Research Foundation DFG within SFB298 'Deformation und Versagen bei metallischen und granularen Strukturen'.

References

1. Alber, H.D.: Initial-Boundary Value Problems for the Inelastic Material Behavior of Metals. Springer Lecture Notes in Mathematics 1682 (1998)
2. Betten, J.: Elastizitäts- und Plastizitätslehre. Vieweg 1986
3. Campbell, S.L., Marszalek, W.: The index of an infinite dimensional implicit system. Report, NCSU Univ., 1996, to appear in Math. Modelling of Systems
4. Chan, K., Bodner, S., Lindholm, U.: Phenomenological Modeling of Hardening and Thermal Recovery in Metals. Journal of Engineering Materials and Technology Vol.110, 1-8 (1988). Phenomenological Modeling of Hardening and Thermal
5. Ciarlet, P.G.: Mathematical Elasticity I. North Holland 1988
6. Eich-Soellner, E., Führer, C.: Numerical Methods in Multibody Dynamics. Teubner 1998
7. Fritzen, P.: Numerische Behandlung nichtlinearer Probleme der Elastizitäts- und Plastizitätstheorie. Diss., TU Darmstadt 1997
8. Hairer, E., Wanner, G.: Solving Ordinary Differential Equations II. 2nd. Ed., Springer 1996
9. Hughes, T.J.: The Finite Element Method. Prentice Hall 1987
10. Jahnke, M., Popp, K., Dirr, B.: Approximate analysis of flexible parts in multibody systems using the finite element method. In Schiehlen W.(Ed.): Advanced Multibody System Dynamics, Kluwer Academic Publishers 1993, pp. 237-256
11. Kikuchi, N., Oden, J.: Conctact Problems in Elasticity. SIAM: Philadelphia 1988
12. Lubich, C.: Integration of stiff mechanical systems by Runge-Kutta methods. ZAMP 44, 1022-1053 (1993)
13. Nordmark, A.: The Matlab PDE Toolbox. The Mathworks Inc., 1995
14. Rheinboldt, W.C., Simeon, B.: On computing smooth solutions of DAEs for elastic multibody systems. Submitted to Comp. Math. Appl.
15. Roberson, R., Schwertassek, R.: Dynamics of Multibody Systems. Springer 1988
16. Scherf, O., Simeon, B.: Viscoplastic Deformation from the DAE Perspective - a Benchmark Problem. Submitted to ZAMM
17. Schiehlen, W.O. (Ed.): Multibody System Handbook. Springer 1990
18. Seibert, T.: Simulationstechniken zur Untersuchung der Streuung bei der Parameteridentifikation inelastischer Werkstoffmodelle, Diss., TU Darmstadt 1996
19. Simeon, B.: MBSPACK - Numerical integration software for constrained mechanical motion. Surv. on Math. in Ind. 5, 169-202 (1995)
20. ˜: Modelling a flexible slider crank mechanism by a mixed system of DAEs and PDEs. Math. Modelling of Systems 2, 1-18 (1996)
21. Stoer, J., Bulirsch, R.: Introduction to Numerical Analysis. Springer 1993
22. Tallec, P. Le: Numerical Methods for Nonlinear Elasticity. In: Ciarlet, P., Lions, J.(eds.): Handbook of Numerical Analysis III. North-Holland 1994
23. Wallrapp, O.: Standardization of flexible body modelling in MBS codes. Mech. Struct. Mach. 22, 283-304 (1994)
24. Washizu, K.: Variational Methods in Elasticity and Plasticity. Pergamon 1982